

DIFFERENTIAL-ALGEBRAIC APPROACH TO COUPLED PROBLEMS OF DYNAMIC THERMOELASTICITY *

WANG Lin-xiang¹, Roderick V. N. Melnik²

(1. MCI, Faculty of Science and Engineering, University of Southern Denmark,
Sonderborg, DK-6400, Denmark;

2. Center for Coupled Dynamics & Complex Systems, Wilfrid Laurier University,
75 University Avenue West, Waterloo, ON, Canada, N2L 3C5)

(Communicated by ZHOU Zhe-wei)

Abstract: An efficient numerical approach for the general thermomechanical problems was developed and it was tested for a two-dimensional thermoelasticity problem. The main idea of our numerical method is based on the reduction procedure of the original system of PDEs describing coupled thermomechanical behavior to a system of Differential Algebraic Equations (DAEs) where the stress-strain relationships are treated as algebraic equations. The resulting system of DAEs was then solved with a Backward Differentiation Formula (BDF) using a fully implicit algorithm. The described procedure was explained in detail, and its effectiveness was demonstrated on the solution of a transient uncoupled thermoelastic problem, for which an analytical solution is known, as well as on a fully coupled problem in the two-dimensional case.

Key words: thermoelasticity; two-dimensional; differential-algebraic solvers

Chinese Library Classification: O343.6; O155

2000 Mathematics Subject Classification: 74F05; 65M99

Digital Object Identifier(DOI): 10.1007/s 10483-006-0905-z

Introduction

Coupling effects, an essential feature of many different physical phenomena, are known difficult to treat numerically, while the existence of analytical solutions to coupled problems is, as a rule, contingent on substantial simplifications of such problems which often lead to models too remote from a realistic physical consideration.

Examples of coupled problems are provided by theory of electromagnetism, magneto-elasticity, electro-elasticity to name just a few areas of what is generically known as coupled field theory^[1]. Thermoelasticity is another example from coupled field theory where two (or more) distinctively different physical fields should be treated in an intrinsic correlation. Although, thermoelasticity was one of the first areas in coupled field theory that attracted the attention of mathematicians (see Ref.[2] and references therein), the interest to the models describing thermomechanical coupling has been revitalised by new important practical problems, including those that are at the cutting edge of the current technological innovations. Some such problems require dealing with intrinsically nonlinear effects such as phase transformations and hysteresis phenomena, while others could be well described by linear models. A unifying factor of all these models is the coupling between mechanical and thermal fields which, on many occasions, keeps a key to the essence of the physical phenomena under consideration. This is the case,

* Received Sep.19, 2005; Revised Jun.17, 2006

Corresponding author WANG Lin-xiang, Associate Professor, Doctor, E-mail: wanglinxiang@mci.sdu.dk

for example, for many complex materials which could exhibit various types of solid-solid phase transformations, as well as for a number of contact problems in dynamic thermoelasticity.

Whether a specific model of thermoelasticity is nonlinear, as it is the case for shape memory alloy problems^[3,4], or linear, as it is the case for other problems of practical interest^[2,5], it is important to emphasize that for many problems dealing with thermomechanical coupling transient, rather than steady-state, behavior of the material is in the focus of interest. To approach the solution of many complex dynamic problems of coupled thermoelasticity it is essential to develop efficient numerical procedures that are able to treat coupled effects for a wide range of time-dependent loading conditions. Several efficient algorithms have been recently proposed in the literature for coupled linear and nonlinear thermoelasticity, and some of those can even deal quite efficiently with strong nonlinearity in shape memory materials (see Refs.[3,6–8] and references therein). However, most of them have been developed for the one-dimensional case, while a generalization of such algorithms to dimensions higher than one is not a trivial task which requires good test examples for validation^[8–10]. For problems with dimensions higher than one, there are few investigations reported in the literature. In Ref.[11], the boundary integral method is applied to the plane theory of elasticity analytically, while in Ref.[15] a particular integral method is applied to 2D and 3D transient potential flow (heat conduction) analysis, and in Ref.[12] a 2D thermoelastic problem is investigated by Laplace and Fourier transform techniques. For numerical analysis, boundary element method is employed for thermoelastic problems in Refs.[13–15] and references therein, the same method is also employed in Ref.[16] for analyzing the thermal and mechanical shock in a 2D domain. But all the methods in these investigations are very specific because either transform techniques or particular integral methods have some special requirements on the features of the problems^[12,13,15].

Therefore, it is the purpose of this paper to develop an efficient approach to the solution of coupled dynamic problems of thermoelasticity, which should be easy to be generalised for more complicated models. The discussion is focused on two-dimensional models. The main idea of our numerical method is based on a reduction procedure of the original system of PDEs to a system of DAEs where the stress-strain relationships are treated as a set of algebraic equations, in a way similar to that proposed in Refs.[3,6]. The resulting system of DAEs are then solved with backward differentiation formulae. This idea is a convenient way to analyze fundamentally different thermomechanical phenomena via a unified computational treatment. The described procedure is explained here in detail for transient coupled thermoelastic problems considered in a two-dimensional finite domain. These problems serve as a test for numerical algorithms developed for the solution of more complicated problems in thermomechanical field such as those dealing with phase transitions in materials with memory.

1 Dynamic Equations for Thermomechanical Coupling

Mathematical models of coupled dynamic thermoelasticity are based on conservation laws for linear momentum and energy. In a quite general setting, the system describing coupled thermomechanical interactions can be written down as follows (*e.g.*, Refs.[6,17]):

$$\begin{cases} \rho \frac{\partial^2 u_i}{\partial t^2} = \nabla_{\mathbf{x}} \cdot \boldsymbol{\sigma} + f_i, & i, j = 1, 2, 3, \\ \rho \frac{\partial e}{\partial t} - \boldsymbol{\sigma}^T : (\nabla \mathbf{v}) + \nabla \cdot \mathbf{q} = g, \end{cases} \quad (1)$$

where ρ is the density of the material, $\mathbf{u} = \{u_i\}_{i=1,2,3}$ is the displacement vector, \mathbf{v} is the velocity, $\boldsymbol{\sigma} = \{\sigma_{ij}\}$ is the stress tensor, \mathbf{q} is the heat flux, e is the internal energy, $\mathbf{f} = (f_1, f_2, f_3)^T$ and g are mechanical and thermal loadings, respectively. Let ϕ be the free energy function of a thermomechanical system described by Eq.(1). Then, stress and the internal

energy function are connected with ϕ by the following relationships:

$$\boldsymbol{\sigma} = \frac{\partial \phi}{\partial \boldsymbol{\eta}}, \quad e = \phi - \theta \frac{\partial \phi}{\partial \theta}, \quad (2)$$

where θ is the temperature, and the Cauchy-Lagrangian strain tensor $\boldsymbol{\eta}$ is given by its components as follows (repeated-index convention is used here):

$$\eta_{ij}(\mathbf{x}, t) = \left(\frac{\partial u_i(\mathbf{x}, t)}{\partial x_j} + \frac{\partial u_j(\mathbf{x}, t)}{\partial x_i} \right) / 2, \quad i, j = 1, 2, 3, \quad (3)$$

where \mathbf{x} are the coordinates of a material point in the domain of interest.

Under an appropriate choice of ϕ , model (1)–(3) can effectively describe linear or nonlinear thermomechanical problems, even such complex nonlinear phenomena as hysteresis and phase transformations in solid materials^[4]. However, in its generality the description of the dynamics of thermomechanical coupling in complicated materials is still only partially known, in particular in the dimensions higher than one. The difficulties in the mathematical treatment of such problems are connected with a complex nonlinear dependencies of the free energy on both mechanical and thermal fields that for the solution of practical problems need to be experimentally validated.

In what follows we limit our consideration to a two-dimensional thermoelastic problem. For the sake of convenience of numerical treatment, the system (1) is rewritten here as the following PDEs:

$$\begin{cases} \frac{\partial u_1}{\partial t} = v_1, & \frac{\partial u_2}{\partial t} = v_2, \\ \rho \frac{\partial v_1}{\partial t} = \frac{\partial \sigma_{11}}{\partial x} + \frac{\partial \sigma_{12}}{\partial y} + f_1, & \rho \frac{\partial v_2}{\partial t} = \frac{\partial \sigma_{12}}{\partial x} + \frac{\partial \sigma_{22}}{\partial y} + f_2, \\ \rho \frac{\partial e}{\partial t} - \boldsymbol{\sigma}^T : (\nabla \mathbf{v}) + \nabla \cdot \mathbf{q} = g. \end{cases} \quad (4)$$

The above equations can be used as a general model for most of the 2D thermomechanical problems, if the algebraic equations for the stress-strain constitutive laws are given. For different problems, different free energy functions should be used, which leads us to different algebraic equations. In the following sections, a differential-algebraic solver is employed for the analysis of system (4) and coupled and uncoupled thermoelastic problems are solved for test.

2 Mathematical Models of Coupled Dynamic Thermoelasticity in 2D Finite Domains

For the 2D thermoelastic problems, the algebraic equations needed to complete the model can be determined according to Eq.(2) by choosing the following free energy function:

$$\phi = -C_v \theta \ln \theta + \frac{1}{2} a_1 e_1^2 + \frac{1}{2} a_2 e_2^2 + \frac{1}{2} a_3 e_3^2 + a_\theta \theta e_2, \quad (5)$$

where C_v is the specific heat of the material, a_i , $i = 1, 2, 3$ and a_θ are the material-specific coefficients, and e_1 , e_2 , e_3 are dilatational, deviatoric, and shear components of strain, respectively. The later are defined as follows:

$$\begin{cases} e_1(x, y, t) = (\eta_{11} + \eta_{22})/\sqrt{2} \\ e_2(x, y, t) = (\eta_{11} - \eta_{22})/\sqrt{2}, \\ e_3(x, y, t) = (\eta_{12} + \eta_{21})/2. \end{cases} \quad (6)$$

The above free energy function is just a simplification of a relatively complicated one used in Refs.[10,18–20], where the phase transformation is in the focus of interest. For the thermoelastic problems considered here, the emphasis is on the coupling effects between mechanical and thermal field, phase transformation will not be included. Therefore only square terms of the strain are kept in the free energy function, and the coupling between mechanical and thermal field is also slightly simplified by using a direct product of temperature and deviatoric strain. Using this free energy function, it is easy to finalize the system (4) into the following form:

$$\left\{ \begin{array}{l} \frac{\partial u_1}{\partial t} = v_1, \quad \frac{\partial u_2}{\partial t} = v_2, \\ \rho \frac{\partial v_1}{\partial t} = \frac{\partial \sigma_{11}}{\partial x} + \frac{\partial \sigma_{12}}{\partial y} + f_1, \quad \rho \frac{\partial v_2}{\partial t} = \frac{\partial \sigma_{12}}{\partial x} + \frac{\partial \sigma_{22}}{\partial y} + f_2, \\ C_v \frac{\partial \theta}{\partial t} = k \frac{\partial^2 \theta}{\partial x^2} + k \frac{\partial^2 \theta}{\partial y^2} + a_\theta \theta \frac{\partial e_2}{\partial t} + g, \\ \sigma_{11} = \frac{\sqrt{2}}{2} a_1 e_1 + \frac{\sqrt{2}}{2} a_2 e_2 + \frac{\sqrt{2}}{2} a_\theta \theta, \\ \sigma_{12} = \frac{1}{2} a_3 e_3, \\ \sigma_{22} = -\frac{\sqrt{2}}{2} a_1 e_1 + \frac{\sqrt{2}}{2} a_2 e_2 + \frac{\sqrt{2}}{2} a_\theta \theta. \end{array} \right. \quad (7)$$

In the above equations, if the material-specific coefficients are chosen as follows:

$$a_1 = \sqrt{2}\mu, \quad a_2 = \sqrt{2}(\lambda + \mu), \quad a_\theta = -\sqrt{2}\gamma, \quad a_3 = a_1, \quad (8)$$

the system (7) would take the following form:

$$\left\{ \begin{array}{l} \frac{\partial u_1}{\partial t} = v_1, \quad \frac{\partial u_2}{\partial t} = v_2, \\ \rho \frac{\partial v_1}{\partial t} = \frac{\partial \sigma_{11}}{\partial x} + \frac{\partial \sigma_{12}}{\partial y} + f_1, \quad \rho \frac{\partial v_2}{\partial t} = \frac{\partial \sigma_{12}}{\partial x} + \frac{\partial \sigma_{22}}{\partial y} + f_2, \\ C_v \frac{\partial \theta}{\partial t} = k \frac{\partial^2 \theta}{\partial x^2} + k \frac{\partial^2 \theta}{\partial y^2} - \theta \gamma \left(\frac{\partial v_1}{\partial x} + \frac{\partial v_2}{\partial y} \right), \\ \sigma_{11} = \mu \left(\frac{\partial u_1}{\partial x} - \frac{\partial u_2}{\partial y} \right) + (\lambda + \mu) \left(\frac{\partial u_1}{\partial x} + \frac{\partial u_2}{\partial y} \right) - \gamma \theta, \\ \sigma_{12} = \mu \left(\frac{\partial u_1}{\partial y} + \frac{\partial u_2}{\partial x} \right), \\ \sigma_{22} = -\mu \left(\frac{\partial u_1}{\partial x} - \frac{\partial u_2}{\partial y} \right) + (\lambda + \mu) \left(\frac{\partial u_1}{\partial x} + \frac{\partial u_2}{\partial y} \right) - \gamma \theta, \end{array} \right. \quad (9)$$

where λ and μ are Lamé's coefficients, γ is stress-temperature modulus (related to the coupling coefficient). It is obvious that all equations in the system (9) are linear, except the energy balance equation because of nonlinear coupling term. For comparison, the nonlinear coupling term is linearized here by replacing the time-dependent temperature θ with the time-independent reference temperature θ_0 . This linearization makes the system (9) exactly the same one as those of 2D linear thermoelastic problems investigated in Refs.[4,5,14,16,21,22]. It is worthy to note that the system (9) is a mixed system containing parabolic and hyperbolic equations. Constitutive laws defining stress-strain relationships are treated here as algebraic equations with respect to strain and temperature. This fact leads us to a computational algorithm that, with minimal modification, allows us to apply it to most of the thermomechanical problems.

3 Numerical Discretisation of Governing Equations

Although the system (9) is a substantially simplified version of the general thermomechanical problems, its analytical treatment is limited by only few known special cases from uncoupled theory of thermoelasticity^[21,22]. It is this problem that is used as the first example for validation of our numerical procedure. Before considering aspects of numerical discretisation, we normalise the system (9) by using the following dimensionless variables:

$$\begin{cases} \hat{x} = x/\alpha, & \hat{t} = tC_1/\alpha, & \hat{\sigma}_{ij} = \sigma_{ij}/(\gamma\theta_0), & \hat{\theta} = (\theta - \theta_0)/\theta_0, \\ \hat{u}_i = (\lambda + 2\mu)u_i/(\alpha\lambda\theta_0), & \hat{v}_i = \frac{\partial \hat{u}_i}{\partial \hat{t}}, & \hat{f}_i = \frac{\alpha}{\gamma\theta_0}f_i, \end{cases} \quad (10)$$

where $\alpha = k/\rho C_v C_1$ is the dimensionless unit length, $C_1 = ((\lambda + 2\mu)/\rho)^{1/2}$ is the velocity of propagation of the longitudinal wave, $\gamma = (3\lambda + 2\mu)\beta$, and β is the thermal expansion coefficient of the material under consideration. After replacing all variables according to Eq.(10) and rearrangement, the system (9) takes the following form (dropping the hat for convenience):

$$\begin{cases} \frac{\partial u_1}{\partial t} = v_1, & \frac{\partial u_2}{\partial t} = v_2, \\ \frac{\partial v_1}{\partial t} = \frac{\partial \sigma_{11}}{\partial x} + \frac{\partial \sigma_{12}}{\partial y} + f_1, & \frac{\partial v_2}{\partial t} = \frac{\partial \sigma_{12}}{\partial x} + \frac{\partial \sigma_{22}}{\partial y} + f_2, \\ \frac{\partial \theta}{\partial t} = \frac{\partial^2 \theta}{\partial x^2} + \frac{\partial^2 \theta}{\partial y^2} - \frac{\theta_0 \gamma^2}{\rho C_v (\lambda + 2\mu)} \left(\frac{\partial v_1}{\partial x} + \frac{\partial v_2}{\partial y} \right), \\ \sigma_{11} = \frac{\lambda}{\lambda + 2\mu} \frac{\partial u_2}{\partial y} + \frac{\partial u_1}{\partial x} - \theta, \\ \sigma_{12} = \frac{\mu}{\lambda + 2\mu} \left(\frac{\partial u_1}{\partial y} + \frac{\partial u_2}{\partial x} \right), \\ \sigma_{22} = \frac{\lambda}{\lambda + 2\mu} \frac{\partial u_1}{\partial x} + \frac{\partial u_2}{\partial y} - \theta. \end{cases} \quad (11)$$

After discretization, the system (11) will be recasted into the following form:

$$\begin{cases} \frac{du_{1,ij}(t)}{dt} = v_{1,ij}(t), & \frac{du_{2,ij}(t)}{dt} = v_{2,ij}(t), \\ \frac{dv_{1,ij}(t)}{dt} = D_x(\sigma_{11,ij}) + D_y(\sigma_{12,ij}) + f_1, \\ \frac{dv_{2,ij}(t)}{dt} = D_x(\sigma_{12,ij}) + D_y(\sigma_{22,ij}) + f_2, \\ \frac{d\theta_{ij}(t)}{dt} = D_{xx}(\theta_{ij}) + D_{yy}(\theta_{ij}) - \frac{\theta_0 \gamma^2}{\rho C_v (\lambda + 2\mu)} (D_x(v_{1,ij}) + D_y(v_{2,ij})), \\ 0 = -\sigma_{11,ij} + \frac{\lambda}{\lambda + 2\mu} D_y(u_{2,ij}) + D_x(u_{1,ij}) - \theta_{ij}, \\ 0 = -\sigma_{12,ij} + \frac{\mu}{\lambda + 2\mu} D_y(u_{1,ij}) + D_x(u_{2,ij}), \\ 0 = -\sigma_{22,ij} + \frac{\lambda}{\lambda + 2\mu} D_x(u_{1,ij}) + D_y(u_{2,ij}) - \theta_{ij}, \end{cases} \quad (12)$$

where $i = 1, 2, \dots, m_x$ and $j = 1, 2, \dots, m_y$ with m_x and m_y being the numbers of discretisation points for discretisation in x - and y -directions, respectively; $z_{ij}(t)$ (where z is one of the eight

unknown functions) denotes the value of function z in the grid point (x_i, y_j) at time t ; D_x (D_y) and D_{xx} (D_{yy}) are first and second central difference derivative operators, respectively.

For the sake of convenience, the system (12) can be recasted into the following form:

$$\mathbf{A} \frac{d\mathbf{U}}{dt} + \mathbf{H}(t, \mathbf{X}, \mathbf{U}) = \mathbf{0}, \quad (13)$$

where $\mathbf{U} = [\mathbf{u}_1, \mathbf{v}_1, \mathbf{u}_2, \mathbf{v}_2, \boldsymbol{\theta}, \boldsymbol{\sigma}_{11}, \boldsymbol{\sigma}_{12}, \boldsymbol{\sigma}_{22}]^T$ is a vector collecting all the unknowns we are solving for, in which \mathbf{u}_1 is a sub-vector collecting the displacement u_1 on all the discretization nodes, and similarly for all other sub-vectors. Matrix $\mathbf{A} = \text{diag}(\mathbf{m}_{u_1}, \mathbf{m}_{v_1}, \mathbf{m}_{u_2}, \mathbf{m}_{v_2}, \mathbf{m}_{\theta}, \mathbf{m}_{\sigma_{11}}, \mathbf{m}_{\sigma_{12}}, \mathbf{m}_{\sigma_{22}})$ collecting the multipliers for the derivative term of all the unknowns, in which the sub-matrix \mathbf{m}_{u_1} is an identity matrix because the multiplier for $\frac{\partial u_1}{\partial t}$ is 1, and similarly the sub-matrices \mathbf{m}_{v_1} , \mathbf{m}_{u_2} , and \mathbf{m}_{θ} are all identity matrices. While those sub-matrices associated with stress components, $\mathbf{m}_{\sigma_{11}}$, $\mathbf{m}_{\sigma_{12}}$, $\mathbf{m}_{\sigma_{22}}$, are all zero, because there are no derivative terms of these variables in terms of time occur in Eq.(12). $\mathbf{H} = [\mathbf{H}_{u_1}, \mathbf{H}_{v_1}, \mathbf{H}_{u_2}, \mathbf{H}_{v_2}, \mathbf{H}_{\theta}, \mathbf{H}_{\sigma_{11}}, \mathbf{H}_{\sigma_{12}}, \mathbf{H}_{\sigma_{22}}]^T$ is a vector collecting all the algebraic functions resulting from spatial discretization for the associated unknowns, in which \mathbf{H}_{u_1} collects the algebraic functions for u_1 on all the discretization nodes by excluding the time derivative terms (actually $\mathbf{H}_{u_1} = -\mathbf{v}_1$ according to the top line in Eq.(12)). All other sub-vectors in \mathbf{H} are defined similarly.

It is obvious that \mathbf{A} is a singular matrix and the system (13) is a stiff system, which means an implicit algorithm has to be chosen to do the time integration. Here the second order backward differentiation formula is employed for the purpose, by which the time derivatives are approximated by the second order backward difference scheme^[5]:

$$\mathbf{A} \left(\frac{3}{2} \mathbf{U}^n - 2\mathbf{U}^{n-1} + \frac{1}{2} \mathbf{U}^{n-2} \right) + \Delta t \mathbf{H}(t_n, \mathbf{X}, \mathbf{U}^n) = \mathbf{0}, \quad (14)$$

where n denotes the current time layer. On each time layer, the above algebraic system can be recasted into the following:

$$\Delta t \mathbf{H}(t_n, \mathbf{X}, \mathbf{U}^n) + \frac{3}{2} \mathbf{A} \mathbf{U}^n = \mathbf{A} \left(-2\mathbf{U}^{n-1} + \frac{1}{2} \mathbf{U}^{n-2} \right), \quad (15)$$

with \mathbf{U}^{n-1} and \mathbf{U}^{n-2} are known. The above system is then converted into a nonlinear algebraic system and can be solved for \mathbf{U}^n by use of Newton's iteration methods.

4 Transient Thermomechanical Analysis with Differential-Algebraic Solvers

The procedure described in Section 3 has been applied to a range of problems describing thermomechanical interactions in solid materials. In this section we consider two such examples. The first example, which was a part of the algorithm validation, deals with a two-dimensional thermoelasticity problem for which an analytical solution is known. The second example is of a general nature, allowing arbitrary thermomechanical loading conditions on a thermoelastic plate. This example deals with a fully coupled time-dependent problem of thermoelasticity.

4.1 Transient problem of thermoelasticity: comparison results with known analytical solutions

First, we consider a unit square plate that is initially at zero temperature and displacements and is subjected to a sudden heat on one of its edges, as depicted in Fig.1(a). We assume that the plate is in plane strain with three of its four lateral sides insulated and restrained from normal displacement while the heated face is maintained at the temperature equal to unity. This problem is a special case of the system (11), and can be described by the following model

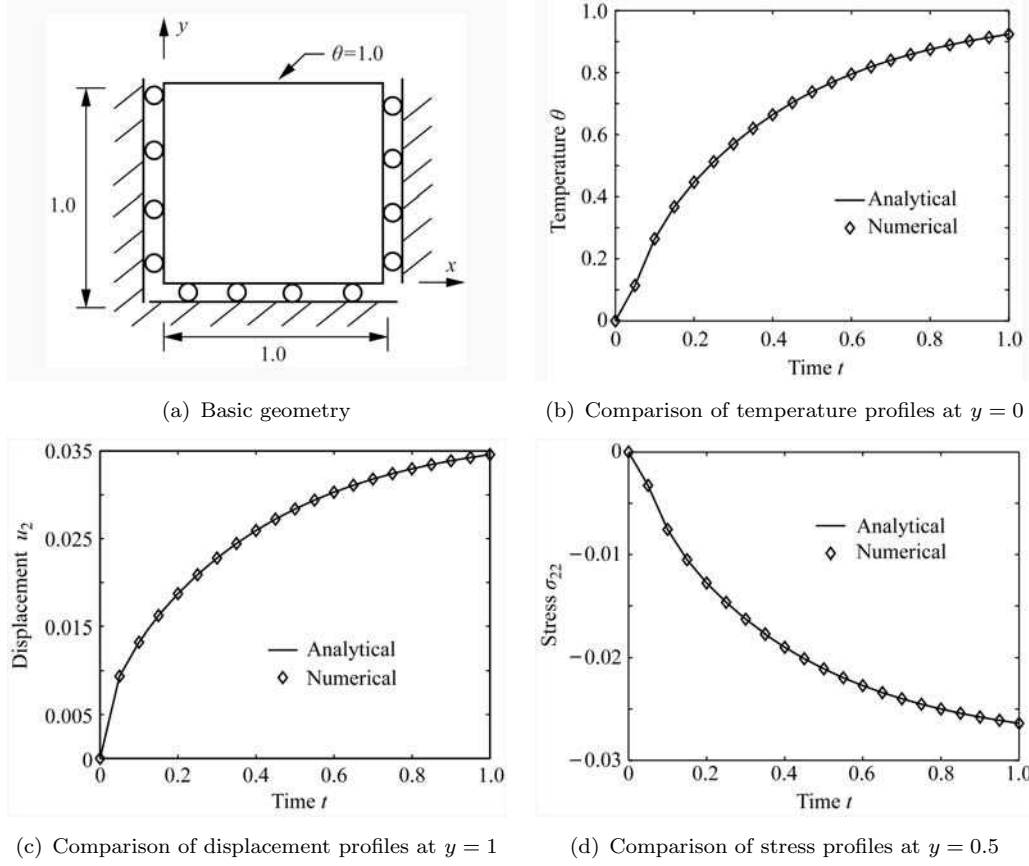


Fig.1 Comparison of numerical and analytical results for the 2D dynamic problem with a suddenly heated sample (from left-to-right, top-to-bottom)

in the steady-state situation:

$$\begin{cases} \frac{\mu}{\lambda + 2\mu} \left(\frac{\partial^2 u_1}{\partial x^2} + \frac{\partial^2 u_1}{\partial y^2} \right) + \frac{\lambda + \mu}{\lambda + 2\mu} \left(\frac{\partial^2 u_1}{\partial x^2} + \frac{\partial^2 u_2}{\partial x \partial y} \right) - \frac{\partial \theta}{\partial x} + f_1 = 0, \\ \frac{\mu}{\lambda + 2\mu} \left(\frac{\partial^2 u_2}{\partial x^2} + \frac{\partial^2 u_2}{\partial y^2} \right) + \frac{\lambda + \mu}{\lambda + 2\mu} \left(\frac{\partial^2 u_1}{\partial x \partial y} + \frac{\partial^2 u_2}{\partial y^2} \right) - \frac{\partial \theta}{\partial y} + f_2 = 0, \\ \frac{\partial \theta}{\partial t} = \frac{\partial^2 \theta}{\partial x^2} + \frac{\partial^2 \theta}{\partial y^2} + g. \end{cases} \quad (16)$$

The system (16) can be solved in an uncoupled manner by first solving the heat conduction equation, and then substituting temperature in the equations of motion. As a result, by assuming the absence of the external thermomechanical loadings ($f_1 = f_2 = g = 0$) the problem just formulated can be solved analytically. This allows us to compare the results obtained with the DAE-based numerical procedure described in Section 3 and the analytical solution, known in this specific case. We choose the following properties of the material for the plate: $\lambda = 0.38461 \text{ kg}/(\text{ms}^2)$, $\mu = 0.576923 \text{ kg}/(\text{ms}^2)$, $\beta = 0.02 \text{ K}^{-1}$ (see also Table (1) for derived variables entering dimensionless system (16)). We are interested in the solution symmetric in the x -direction. Following the well-known procedure (*e.g.*, Refs.[14,22]) we get

$$\begin{cases} \theta(y, t) = 1 - \frac{4}{\pi} \sum_{n=0}^{\infty} \frac{(-1)^n}{2n+1} \exp\left(-\frac{(2n+1)\pi^2 t}{4}\right) \cos\left(\frac{(2n+1)\pi y}{2}\right), \\ u_2(y, t) = \frac{(1+\nu)\beta}{(1-\nu)} \int_0^y \theta(y, t) dy, \\ \sigma_{22}(y, t) = -\frac{\beta E}{(1-\nu)} \theta(y, t). \end{cases} \quad (17)$$

We compared the solution obtained analytically with that obtained by the numerical procedure described in Section 3. Note that the solution is uniform in the x -direction due to the symmetry. This fact is reflected in the analytical representation of the solution (17). The system (16) has been discretised as on an 11×41 grid by using the procedure described in the previous section. Computations presented in Fig.1 were obtained with time step size 2×10^{-3} . In Fig.1(b) we present the temperature variation at the center point on the bottom edge of the square plate. Figure 1(c) gives vertical displacement profiles of the center point on the top edge, and Fig.1(d) gives the variation of lateral stress at the center of the unit square plate. The results of the numerical solution obtained with the proposed methodology is practically un-distinguishable from the analytical solution depicted on the same plots.

Table 1 Dimensionless parameters and thermomechanical loading conditions for computational experiments

| Parameters | Value | Parameters | Value |
|---|--|------------------------------|---|
| $C = \theta_0 \gamma^2 / (\rho c_e (\lambda + 2\mu))$ | 0, 0.1 | $\lambda / (\lambda + 2\mu)$ | 0.3 |
| $\mu / (\lambda + 2\mu)$ | 0.4 | Time span | $t \in [0, 6]$ |
| Number of nodes in x | 41 | Number of nodes in y | 21 |
| Time step size | 0.005 | Loading in Case 1 | $\theta(t) = 5te^{-2t}, \sigma_n = 0$ |
| Loading in Case 2 | $\sigma_{11}(t) = 5te^{-2t}, \frac{\partial \theta}{\partial x} = 0$ | Loading in Case 3 | $\sigma_{11}(t) = 5te^{-2t}, \theta(t) = 5te^{-2t}$ |

4.2 Fully coupled dynamic problem of thermoelasticity

Now, we are in a position to consider a fully coupled dynamic problem of thermoelasticity with thermomechanical loadings. We consider a square plate subjected to the following boundary conditions (see Fig.2(a)):

$$u_1 = u_2 = 0, \quad \frac{\partial \theta}{\partial x} = 0, \quad \text{at } x = 10; \quad (18)$$

$$\frac{\partial u_1}{\partial y} = \frac{\partial u_2}{\partial y} = 0, \quad \frac{\partial \theta}{\partial y} = 0, \quad \text{at } y = \pm 5, \quad (19)$$

with the same initial conditions as before. A set of numerical experiments have been conducted for this problem which is described by the model (11). The type of boundary conditions imposed at $x = 0$ is experiment-specific, and we discuss them as appropriate in the text. In order to compare the results of computation for the fully coupled and uncoupled cases we introduce the modified coupling coefficient as

$$C = \frac{\theta_0 \gamma^2}{\rho C_v (\lambda + 2\mu)}. \quad (20)$$

Other computational parameters of interest and patterns of thermomechanical loadings in Cases 1–3 discussed below are given in Table 1. The results presented below have been compared to the known results computed with the boundary element method (*e.g.*, Refs.[4,16], for this reason we choose in this problem $l = 10$) where a semi-infinite in x and infinite in y plate has been analysed. According to the system (11) we have computed eight functions of interest:

two displacements, two velocities, and three stress components, as well as the temperature field distribution. Here we present results for temperature, displacements, and stresses for three distinctively different patterns of thermomechanical loading which we consider below.

Case 1: Isolated thermal shock conditions In this case an instantaneous thermal loading is applied to the sample at the edge $x = 0$. The normal derivatives of displacement components at that edge are set to be zero. The applied thermal shock as a function of time is given in Table 1. Under these loading conditions we analyse numerically the displacement component u_1 , the axial stress component σ_{11} , and the thermal field as functions of x and t . Results presented in Fig.2 are given for two moments of dimensionless time, $t = 3$ and $t = 6$. Figure 2(b) shows the distribution of the axial displacements along the x -axis. The influence of the thermal shock on displacements is pronounced in this case due to the coupling between mechanical and thermal fields induced by the shock. In Fig.2(c) we present the temperature distributions for both coupled and uncoupled situations. Again, the effect of coupling is clearly pronounced in the amplitude of thermal profiles as well as in thermal gradients which become steeper in the coupled case. Finally, in Fig.2(d) we present results of computing axial stresses along x -direction. The wave fronts at both analysed moments of time, $t = 3$ and $t = 6$, are resolved well with a relatively small number of grid points used. The amplitude of oscillations in the coupled case is smaller due to a damping effect of the thermal field coupled to the mechanical field. In this case, the coupling effect acts like a damper for this thermomechanical system.

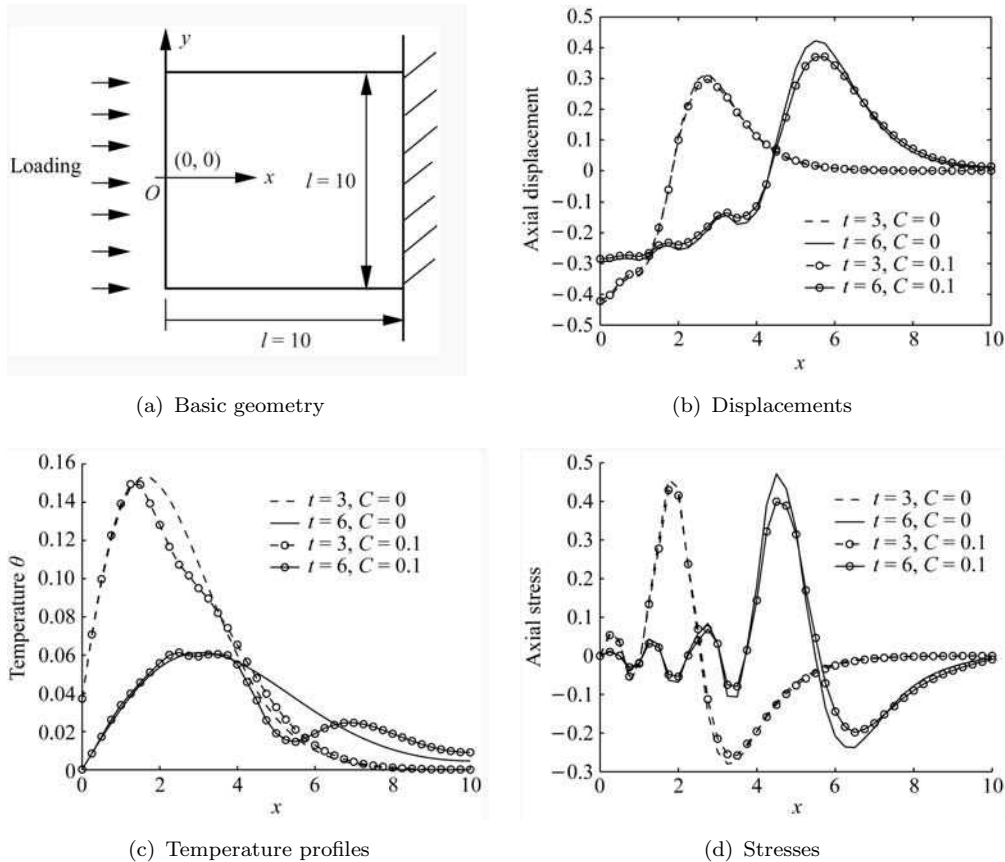
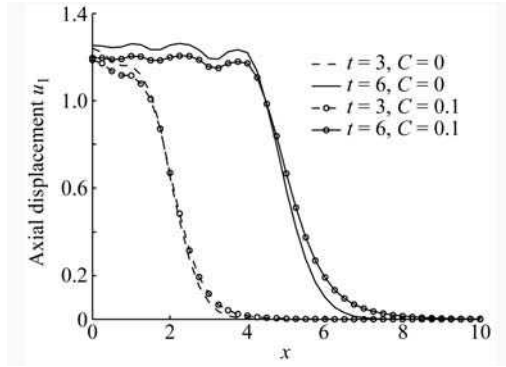
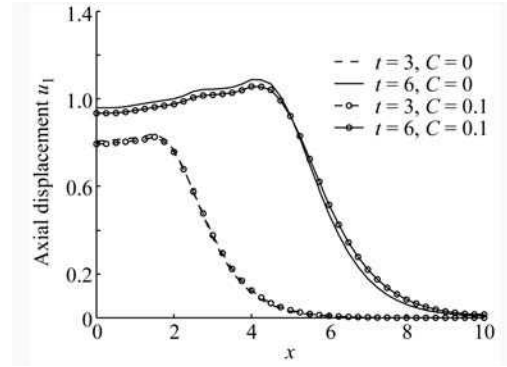


Fig.2 Comparison of numerical and analytical results for the 2D non-dimensional dynamic problem with a sample subjected to thermal loadings

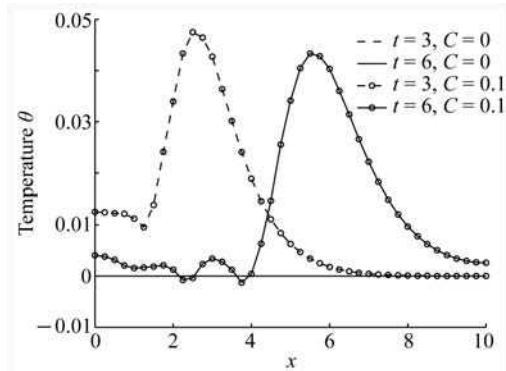
Case 2: Mechanical shock conditions We turn our attention now to a situation where the thermomechanical energy exchange in the system is induced by a time-dependent pressure shock. In particular, we apply a time-dependent normal stress to the edge $x = 0$ of the sample, leaving that edge thermally insulated, and setting the normal derivative of u_2 to zero (see Table 1 for detail). The results of computations are presented in Figs.3(a)–3(c). The analysis of



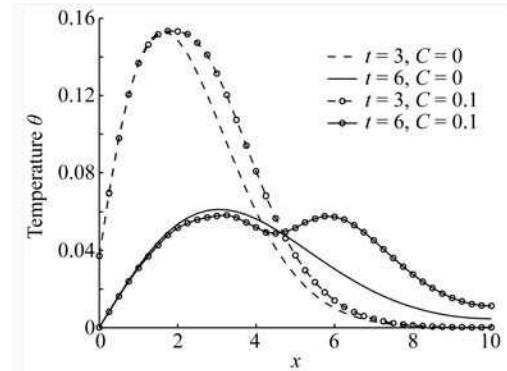
(a) Displacements under pressure shock



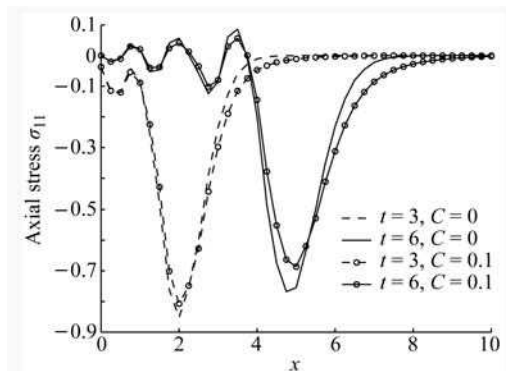
(d) Displacements under coupled thermomechanical shock



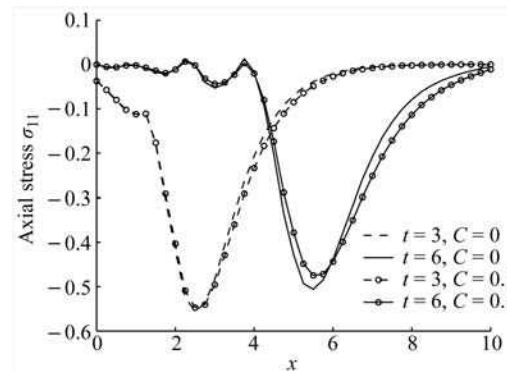
(b) Temperature profiles under pressure shock



(e) Temperature profiles under coupled thermomechanical shock



(c) Stresses under pressure shock



(f) Stresses under coupled thermomechanical shock

Fig.3 Comparison of numerical and analytical results for the 2D non-dimensional dynamic problem with a sample subjected to mechanical and thermomechanical loadings

displacements (Fig.3(a)) and stresses (Fig.3(c)) for different moments of time underline a time-dependent character of the problem in both coupled and uncoupled cases. As for the temperature field in this case, note that since there is no energy input or converted into thermal field in the uncoupled case the temperature is uniform zero. This is not the case in the coupled model as demonstrated by Fig.3(b). Moreover, the peak of the temperature distribution is moving simultaneously with the peak of the compressive axial stresses, as a result of the coupling effect.

Case 3: Combined thermomechanical shock In this case we apply to the edge $x = 0$ time-dependent mechanical and thermal conditions as specified in Table 1. As we expect, the result of this is a superposition of the solutions obtained in Cases 1 and 2. This is demonstrated by Figs.3(d)–3(f). Finally note (see Fig.3(e)) that the effect of coupling speeds up thermal diffusion. Again, this is expected for it is known that the largest amount of the thermomechanical energy transfer takes place in the vicinity of wave fronts.

5 Conclusion

In the present paper, a differential algebraic approach has been developed for the investigation of the dynamics of general thermomechanical problems. The approach has been tested for two 2D thermoelastic problems. Comparison of the present numerical results for a uncoupled 2D thermoelastic problem to the analytical results has been made, and the comparison of the present numerical result for a fully coupled 2D thermoelastic problem to the one computed with boundary element method has also been made.

It has been shown clearly that the differential algebraic approach is efficient for analysis of dynamics of thermoelastic problems. From the reduction procedure, it has been shown that only those algebraic equations need to be modified for different thermomechanical problems, which makes the numerical approach applicable with slight modification in many cases. At the same time, the numerical experiments have shown that stress boundary conditions are easy to be implemented in the current approach because the stress-strain relations are kept as algebraic equations in the model.

References

- [1] Melnik R V N. Convergence of the operator-difference scheme to generalised solutions of a coupled field theory problem[J]. *J Difference Equations Appl*, 1998, **4**(2):185–212.
- [2] Melnik R V N. Discrete models of coupled dynamic thermoelasticity for stress-temperature formulations[J]. *Appl Math Comput*, 2001, **122**(2):107–132.
- [3] Melnik R V N, Roberts A J, Thomas K A. Coupled thermomechanical dynamics of phase transitions in shape memory alloys and related hysteresis phenomena[J]. *Mechanics Research Communications*, 2001, **28**(6):637–651.
- [4] Melnik R V N, Roberts A J, Thomas K A. Phase transitions in shape memory alloys with hyperbolic heat conduction and differential algebraic models[J]. *Computational Mechanics*, 2002, **29**(1):16–26.
- [5] Strunin D V, Melnik R V N, Roberts A J. Coupled thermomechanical waves in hyperbolic thermoelasticity[J]. *J Thermal Stresses*, 2001, **24**(2):121–140.
- [6] Melnik R V N, Roberts A J, Thomas K A. Computing dynamics of copper-based SMA via center manifold reduction of 3D models[J]. *Computational Material Science*, 2000, **18**(3/4):255–268.
- [7] Niezgodka M, Sprekels J. Convergent numerical approximations of the thermomechanical phase transitions in shape memory alloys[J]. *Numer Math*, 1991, **58**:759–778.
- [8] Rawy E K, Iskandar L, Ghaleb A F. Numerical solution for a nonlinear, one-dimensional problem of thermoelasticity[J]. *J Comput Appl Math*, 1998, **100**(1):53–76.
- [9] Abd-Alla A N, Ghaleb A F, Maugin G A. Harmonic wave generation in nonlinear thermoelasticity[J]. *Internat J Engng Sci*, 1994, **32**(7):1103–1116.

-
- [10] Jiang S. Numerical solution for the Cauchy problem in nonlinear 1-D thermoelasticity[J]. *Computig*, 1993, **44**(2):147–158.
 - [11] Abou-Dina M S, Ghaleb A F. On the boundary integral formulation of the plane theory of elasticity with applications (analytical aspects)[J]. *Journal of Computational and Applied Mathematics*, 1999, **106**(1):55–70.
 - [12] Sherief H H, Megahed F A. A two-dimensional thermoelasticity problem for a half space subjected to heat sources[J]. *Internat J Solid and Structure*, 1999, **36**(9):1369–1382.
 - [13] Banerjee P K. The Boundary Element Methods in Engineering[M]. McGraw-Hill, London, 1994, 1–100.
 - [14] Park K H, Banerjee P K. Two- and three-dimensional transient thermoelastic analysis by BEM via particular integrals[J]. *Internat J Solids and Structures*, 2002, **39**:2871–2892.
 - [15] Yang M T, Park K H, Banerjee P K. 2D and 3D transient heat conduction analysis by BEM via particular integrals[J]. *Comput Methods Appl Mech Engrg*, 2002, **191**(15/16):1701–1722.
 - [16] Hosseini-Tehrani P, Eslami M R. BEM analysis of thermal and mechanical shock in a two-dimensional finite domain considering coupled thermoelasticity[J]. *Engineering Analysis with Boundary Elements*, 2000, **24**(3):249–257.
 - [17] Pawlow I. Three-dimensional model of thermomechanical evolution of shape memory materials[J]. *Control and Cybernetics*, 2000, **29**(1):341–365.
 - [18] Ichitsubo T, Tanaka K, Koiva M, Yamazaki Y. Kinetics of cubic to tetragonal transformation under external field by the time-dependent Ginzburg-Landau approach[J]. *Phys Rev B*, 2000, **62**(9):5435–5441.
 - [19] Jacobs A E. Solitons of the square-rectangular martensitic transformation[J]. *Phys Rev B*, 1985, **31**(9):5984–5989.
 - [20] Jacobs A E. Landau theory of structures in tetragonal-orthorhombic ferroelastics[J]. *Phys Rev B*, 2000, **61**(10):6587–6595.
 - [21] Chen J, Dargush G F. BEM for dynamic poroelastic and thermoelastic analysis[J]. *J Solids Struct*, 1995, **32**(15):2257–2278.
 - [22] Timoshenko S P, Goodier J N. Theory of Elasticity[M]. 3rd Edition. McGraw-Hill, New York, 1970, 421–480.
 - [23] Hairer E, Norsett S P, Wanner G. Solving Ordinary Differential Equations II-Stiff and Differential Algebraic Problems[M]. Springer-Verlag, Berlin, 1996, 210–250.
 - [24] Jiang S. On global smooth solutions to the one-dimensional equations of nonlinear inhomogeneous thermoelasticity[J]. *Nonlinear Analysis*, 1993, **20**(10):1245–1256.